Analyzing power in nucleon-deuteron scattering and three-nucleon forces

S. Ishikawa

Department of Physics, Hosei University, 2-17-1 Fujimi, 102-8160 Tokyo, Japan
and Frontier Research Center for Computational Sciences, Science University of Tokyo, 2641 Yamazaki, Noda,
278-8510 Chiba, Japan

Three-nucleon forces have been considered to be one possibility to resolve the well-known discrepancy between experimental values and theoretical calculations of the nucleon analyzing power in low energy nucleon-deuteron scattering. In this Rapid Communication, we investigate the possible effects of two-pion exchange three-nucleon forces on the analyzing power and the differential cross section. We found that the reason for different effects on the analyzing power by different three-nucleon forces found in previous calculations is related to the existence of the contact term. Effects of some variations of two-pion exchange three-nucleon forces are investigated. Also, an expression for the measure of the nucleon analyzing power with quartet P-wave phase shifts is presented. [S0556-2813(99)50403-2]

Differential cross sections for nucleon-deuteron elastic scattering have peaks at forward and backward scattering angles and a minimum at a c.m. scattering angle of, e.g., $\theta \sim 105°$ at $E_{\mathrm{Lab}}^N = 3$ MeV. Around the cross section minimum angle, some observables calculated with realistic nucleon-nucleon (NN) potentials are known to deviate systematically from experimental values [1]. The nucleon analyzing power $A_y(\theta)$ for energies below ≈ 30 MeV has exhibited a notable discrepancy [2,3], which is referred to as the $A_y(\theta)$ puzzle. E.g., in the neutron-deuteron (n-d) elastic scattering at $E_{\mathrm{Lab}}^n = 3$ MeV, experimental $A_y(\theta)$ has a maximum value at $\theta \sim 105°$ [4], while theoretical calculations with modern realistic NN potentials [5–7] undershoot the value by about 30%. The three-nucleon (3N) system has been considered as a good testing ground for the NN interaction. The discrepancy between the experimental and calculated $A_y(\theta)$ may show that there is room for improvement of modern NN potentials. Actually, it was pointed out that changes in ^3P_J NN forces or the spin-orbit component of a potential cause a dramatic increase in $A_y(\theta)$ [8–11]. However constraint from NN observables made it difficult to obtain reasonable changes in the NN potential to resolve the $A_y(\theta)$ puzzle [12–14].

Another possibility for resolving the $A_y(\theta)$ puzzle is the introduction of a three-nucleon force (3NF) into the nuclear Hamiltonian. It is well known that most realistic NN forces underbind the triton, and a 3NF based on the exchange of two pions among the three nucleons (2πE-3NF) can explain the needed attraction. So far, several 2πE-3NF models have been proposed, among which the Tucson-Melbourne (TM) 3NF [15] and the Brazil (the earlier version, BR′ [16], and the latter version, BR [17]) 3NF have been used for 3N calculations. Although these 3NF models were made based on different ideas in constructing off-shell πN scattering amplitudes, which are important ingredients in 2πE-3NF, the resulting potentials have essentially the same form with slightly different parameters. It is reported that with introducing the TM-3NF or BR-3NF, the calculated $A_y(\theta)$ decreases, which means that the discrepancy with the experi-

mental value is enhanced [18,19]. On the other hand, the calculations with the BR′-3NF or another 3NF model, the Urbana (UR) 3NF, are reported to improve $A_y(\theta)$ slightly [20,21]. The UR-3NF is based on the Δ-mediated two-pion exchange diagram [22], which is a part of the diagrams included in TM-3NF and BR-3NF. The discrepancy of the effects on $A_y(\theta)$ should arise from a structure difference between TM/BR-3NF and BR′/UR-3NF. In this Rapid Communication, we study effects of the 2πE-3NF on $A_y(\theta)$ carefully and investigate the possibility of resolving the $A_y(\theta)$ puzzle with a 3NF. All calculations are performed at $E_{\mathrm{Lab}}^n = 3$ MeV, where experimental data are available for the differential cross section [23] and $A_y(\theta)$ [4]. The Argonne V_{18} model (AV18) [6] is used as the input NN potential throughout this Rapid Communication.

Our method for calculating the 3N continuum state is based on a natural extension of the bound state calculation [24,25,19], in which the Faddeev equation is expressed as an integral equation in coordinate space. In the continuum state calculation, there appear additional singularities in the Faddeev integral kernel, which are absent in the bound state calculation: elastic singularity and three-body breakup singularity. The latter does not appear at energies below the three-body breakup threshold as in the present work. The former singularity can be easily treated by the usual subtraction method [26]. In the present calculation, 3N partial wave states for which NN and 3N forces act, are restricted to those with total two-nucleon angular momenta $j \leq 2$. The total 3N angular momenta (J) is truncated at $J = 19/2$, while 3NF is switched off for 3N states with $J \geq 9/2$. These truncating procedures are known to be valid for the low-energy ($E_{\mathrm{Lab}}^n = 3$ MeV) n-d scattering.

The two-pion exchange three-nucleon potential has the following form in momentum space:

$$V(\mathbf{q},\mathbf{q}') = \frac{1}{(2\pi)^6}\left(\frac{f_\pi}{\mu}\right)^2 \frac{F(q^2)}{q^2+\mu^2}\frac{F(q'^2)}{q'^2+\mu^2}(\boldsymbol{\sigma}_1\cdot\mathbf{q})(\boldsymbol{\sigma}_2\cdot\mathbf{q}')$$

$$\times[(\vec{\tau}_1\cdot\vec{\tau}_2)\{a+b(\mathbf{q}\cdot\mathbf{q}')+c(q^2+q'^2)\}$$

$$+(i\vec{\tau}_3\cdot\vec{\tau}_2\times\vec{\tau}_1)(i\boldsymbol{\sigma}_3\cdot\mathbf{q}\times\mathbf{q}')d], \qquad (1)$$

TABLE I. Various parameters for the three-nucleon potentials, Eq. (1), used in the present work.

3NF	$a(\mu^{-1})$	$b(\mu^{-3})$	$c(\mu^{-3})$	$d(\mu^{-3})$
BR$'$	-1.05	-2.29	0.00	-0.768
BR	1.05	-2.29	1.05	-0.768
BR$_\Delta$	0.00	-1.49	0.00	-0.373

where $\mathbf{q}$ and $\mathbf{q}'$ are the momenta of the propagating pions, μ is the pion mass, and $F(q^2)$ a form factor which is parametrized as the dipole form with a cutoff mass Λ. The parameters, a, b, c, and d, for the BR$'$-3NF [16] and the BR-3NF [17] are shown in Table I. Since the Brazil 3NF model is based on the effective Lagrangian approach, in which several diagrams are considered explicitly, we can separate out the 3NF component which results from the Δ-mediated diagram. The parameters for this 3NF component, which should correspond to the UR-3NF, are shown in Table I as BR$_\Delta$.

The cutoff mass Λ is chosen so as to reproduce the triton binding energy. The value of 700 MeV is used for the BR$'$-3NF and the BR-3NF, and 800 MeV for the BR$_\Delta$-3NF. Hereafter these are designated as BR$'_{700}$, BR$_{700}$, and BR$_{\Delta,800}$, respectively.

In general, analyzing powers are defined as a difference between cross sections with different orientations of incoming particles normalized to unpolarized cross sections. Therefore, before discussing the n-d polarization observables, we make a comment on effects of a 3NF on the unpolarized n-d differential cross section (DCS). From calculations for various combinations of NN potentials and 3NF models, we found that the calculated values of the DCS around the minimum region ($\theta = 105°$) have a correlation with those of the triton binding energy B_3. This is shown in Fig. 1, where we plot the calculated values of the DCS($105°$) for $E^n_{\text{Lab}} = 3$ MeV against the calculated B_3. The n-d DCS consists of spin-doublet scattering, spin-quartet scattering, and their interference terms [27]. The above correlation can be understood as a result of the well known relation between the doublet scattering length (^2a) and B_3:
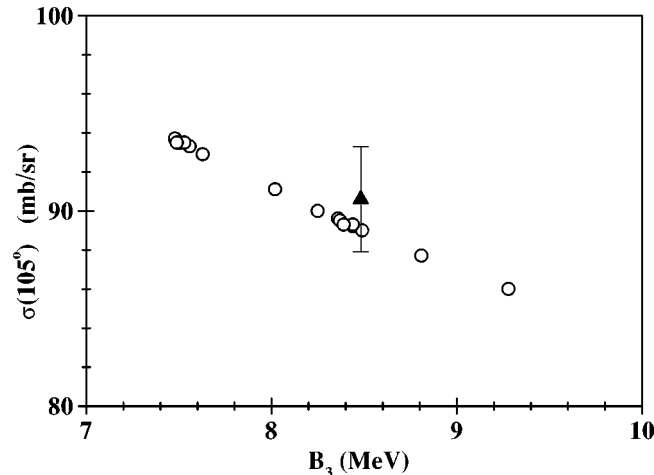

FIG. 1. Calculated values of the n-d differential cross section at $\theta = 105°$ for $E^n_{\text{Lab}} = 3$ MeV plotted against the calculated triton binding energy B_3. The experimental value is taken from Ref. [23].

TABLE II. The results of the triton binding energy; the neutron analyzing power and the differential cross section at $\theta = 105°$ for the n-d scattering at $E^n_{\text{Lab}} = 3$ MeV with AV18+various 3NF and the modified AV18 (Mod-AV18). Experimental values are $A_y(104.0°)$ [4] and $\sigma(103.9°)$ [23].

	B_3 (MeV)	$A_y(105°)$ (%)	$\sigma(105°)$ (mb/sr)
Expt.	8.48	5.96 ± 0.13	90.6 ± 2.7
AV18	7.51	4.29	93.5
AV18+BR$'_{700}$	8.44	4.50	89.2
AV18+BR$_{700}$	8.36	3.62	89.6
AV18+BR$_{\Delta,800}$	8.37	4.43	89.5
Mod-AV18	7.53	5.11	93.4

the Phillips plot. The S-wave DCS at low-energy is proportional to $1/(k^2 + 1/a^2)$, where a is the scattering length and k is the momentum, which means that the DCS decreases if the scattering length a becomes smaller. In fact, the calculated value of the doublet scattering length, 1.35 fm for AV18 ($B_3 = 7.51$ MeV), turns out to be 0.68 fm for AV18+BR$_{700}$ ($B_3 = 8.36$ MeV), while the quartet scattering length is unaffected by a 3NF. Thus the decrease of the DCS with the introduction of a 3NF should be attributed to the reproduction of the triton binding energy. In Fig. 1, we observe that with the reproduction of B_3, the DCS($105°$) gets closer to the central value of the experiment. However, due to a rather large error bar, it is not conclusive whether the decrease is favored.

In Table II, calculated values of B_3; $A_y(105°)$ and DCS($105°$) at $E^n_{\text{Lab}} = 3$ MeV are shown for AV18, AV18+BR$'_{700}$, AV18+BR$_{700}$, and AV18+BR$_{\Delta,800}$, together with the corresponding experimental values, $A_y(\theta)$ at $\theta = 104.0°$ [4] and DCS at $\theta = 103.9°$ [23]. We observe a slight decrease (increase) of $A_y(105°)$ for AV18+BR$_{700}$ (AV18+BR$'_{700}$ and AV18+BR$_{\Delta,800}$) compared to AV18, which is consistent with previous calculations [18–21]. In Table II, results for a modified version of AV18 (Mod-AV18) [10], in which factors 0.96, 0.98, and 1.06 multiply the $^3P_0$, $^3P_1$, and $^3P_2$ AV18 potentials, respectively, are also shown. The modification causes relatively large effects on NN analyzing power: overshooting of peak values of neutron-proton $A_y(\theta)$ by about 30% and 10% for $E^n_{\text{Lab}} = 3$ MeV and 25 MeV, respectively, which has been strongly criticized [13].

The BR-3NF and the BR$_\Delta$-3NF give opposite $A_y(\theta)$ effects. From Table I, we see that there is no term corresponding to the coefficients a and c in the BR$_\Delta$-3NF, which comes from the πN S-wave scattering amplitude. Thus it is interesting to see how each term in 2πE-3NF affects $A_y(\theta)$. To see this, we calculate the n-d scattering at $E^n_{\text{Lab}} = 3$ MeV taking into account each term corresponding to the parameter a, or b, or c, or d in BR$_{700}$ in addition to AV18. Each potential is designated as BR$_a$, BR$_b$, BR$_c$, and BR$_d$, respectively. The results are shown in Table III. From Table III, we see that $A_y(105°)$ decreases for BR$_a$, BR$_c$, and BR$_d$, but increases for BR$_b$. Especially BR$_c$ gives a large $A_y(105°)$ effect. From this, it is concluded that the contribution from BR$_b$ is larger than the one from the other terms in BR$'$-3NF, BR$_\Delta$-3NF, and UR-3NF to give a small increase in $A_y(\theta)$,

TABLE III. The results of the triton binding energy; the neutron analyzing power and the differential cross section at $\theta = 105°$ for the n-d scattering at $E_{\text{Lab}}^n = 3$ MeV with AV18+each term in BR-3NF.

	B_3 (MeV)	$A_y(105°)$ (%)	$\sigma(105°)$ (mb/sr)
AV18+BR$_a$	7.48	4.17	93.7
AV18+BR$_b$	8.25	4.55	90.0
AV18+BR$_c$	7.56	3.81	93.3
AV18+BR$_d$	7.63	4.14	92.9

while the contribution from BR$_c$ is overwhelming in lowering $A_y(\theta)$ in BR-3NF and TM-3NF. The BR$_c$ includes the so-called contact term, which was argued to be excluded to avoid an odd behavior of the 3NF at short range [17], or from a viewpoint of chiral constraints [28]. It is noted that BR$'$-3NF is obtained from BR-3NF with a prescription to remove the contact term: replacing the coefficient a by $a - 2\mu^2 c$ and setting c to zero. Therefore we may express that the different $A_y(\theta)$ effect of BR-3NF from that of BR$'$-3NF arises from the existence of the contact term.

In the AV18+BR$'_{700}$ (AV18+BR$_{\Delta,800}$) calculation, the DCS($105°$) decreases by 5% (4%) compared to the AV18 calculation, while $A_y(105°)$ increases by 5% (3%). On the other hand, in the Mod-AV18 calculation, $A_y(105°)$ increases with little change in the DCS($105°$). Thus there is an essential difference between effects on $A_y(\theta)$ from the 2πE-3NF and from the modification of the ^3P_J NN force. The former is an increase in $A_y(\theta)$ simply due to the decrease of the DCS due to the effect of reproducing the triton binding energy.

In Table III, we observe that each term in BR-3NF gives quite different effects in $A_y(\theta)$. Next, we investigate each effect of the four terms in the 2πE-3NF. To do so, we introduced only the a (b, c, d)-term as a 3NF by varying the coefficient of a (b, c, d) to reproduce the triton binding energy. These 3NF models are designated as W_a, W_b, W_c, and W_d. The results are shown in Table IV together with the values of the coefficients. Although the change of sign in a and c, and of the magnitude in a compared to the original values in Table I may be unnatural, these 3NF models might be useful as phenomenological ones which reproduce the triton binding energy within a restricted functional form. A

TABLE IV. The results of the triton binding energy; the neutron analyzing power and the differential cross section at $\theta = 105°$ for the n-d scattering at $E_{\text{Lab}}^n = 3$ MeV with AV18+W_a, W_b, W_c, and W_d.

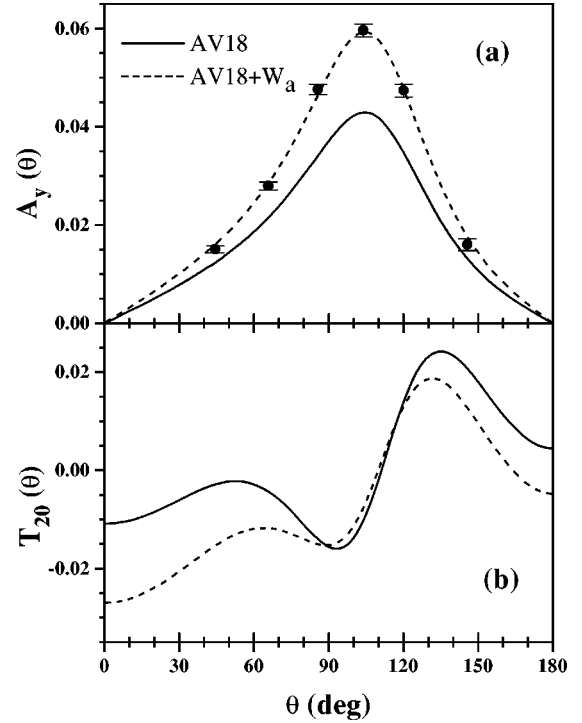|	B_3 (MeV)	$A_y(105°)$ (%)	$\sigma(105°)$ (mb/sr)
AV18+W_a ($a = -14.4\mu^{-1}$)	8.49	5.93	89.0
AV18+W_b ($b = -2.90\mu^{-3}$)	8.50	4.64	89.0
AV18+W_c ($c = -1.25\mu^{-3}$)	8.49	5.13	88.8
AV18+W_d ($d = -3.10\mu^{-3}$)	8.50	3.65	88.9

FIG. 2. $A_y(\theta)$ at $E_{\text{Lab}}^n = 3$ MeV (a) and $T_{20}(\theta)$ at $E_{\text{Lab}}^d = 6$ MeV (b) calculated with AV18 (solid lines) and AV18+W_a (dashed lines). Experimental data of $A_y(\theta)$ are taken from Ref. [4].

variety of $A_y(\theta)$ effects are observed from these 3NF models: a large increase due to W_a; a small increase due to W_b and W_c; a relatively large decrease due to W_d, besides the decrease of in the DCS($105°$) due to the binding energy effect. It is remarkable that W_a seems to reproduce the experimental value of $A_y(105°)$ quite well. However, it turns out that the deuteron tensor analyzing powers are modified improperly by W_a at the same time. In Fig. 2, we plot $A_y(\theta)$ at $E_{\text{Lab}}^n = 3$ MeV (a) and $T_{20}(\theta)$ at $E_{\text{Lab}}^d = 6$ MeV (b) calculated with AV18 (solid lines) and AV18+W_a (dashed lines). We see that the experimental data for $A_y(\theta)$ are well reproduced with the introduction of W_a, and $T_{20}(\theta)$ is significantly modified. Although there is no $T_{20}(\theta)$ data for n-d scattering, recent precise measurements of tensor analyzing powers for proton-deuteron scattering are reported to be well reproduced by calculations without a 3NF [29]. Thus such distortion of $T_{20}(\theta)$ for n-d scattering may produce another ''puzzle.''

It is found that the W_a-3NF gives a different effect on n-d polarization observables than other 3NF models. We remark that this difference can be seen in the n-d quartet P-wave phase-shifts: $\delta_{4P_{1/2}}$, $\delta_{4P_{3/2}}$, and $\delta_{4P_{5/2}}$, to which $A_y(\theta)$ is known to be sensitive. The relation between the n-d phase shifts and $A_y(\theta)$ is quite complicated, but as derived in the Appendix, a combination

$$-4M_{4P_{1/2}} - 5M_{4P_{3/2}} + 9M_{4P_{5/2}} \qquad (2)$$

appears in an expression for $A_y(\theta)$, where $M_{4P_J} = \exp(i\delta_{4P_J})\sin(\delta_{4P_J})$. For small phase shift differences, Eq. (2) is proportional to

TABLE V. Phase shift for the n-d $^4P_{1/2}$ state and the differences $\Delta_{3/2-1/2}$ and $\Delta_{5/2-3/2}$, which are defined in the text, at $E_{Lab}^n = 3$ MeV.

	$\delta_{4P_{1/2}}$	$\Delta_{3/2-1/2}$	$\Delta_{5/2-3/2}$
AV18	24.2	1.9	0.1
AV18+BR$_{700}$	24.5	1.9	-0.2
AV18+BR$'_{700}$	24.6	1.4	0.4
AV18+BR$_{\Delta,800}$	24.5	1.6	0.3
Mod-AV18	24.0	2.2	0.2
AV18+W_a	24.9	0.2	1.4

$$4\Delta_{3/2-1/2}+9\Delta_{5/2-3/2}, \qquad (3)$$

where $\Delta_{J-J'}=\delta_{4P_J}-\delta_{4P_{J'}}$. Equation (3) is a convenient expression for $A_y(\theta)$ being consistent with results of three-nucleon phase shift analysis [10]. In Table V, we list the calculated values of $\delta_{4P_{1/2}}$, $\Delta_{3/2-1/2}$, and $\Delta_{5/2-3/2}$ for some models presented in this work. From Table V we see that $\Delta_{5/2-3/2}\sim 0$ for most cases except for W_a, for which $\Delta_{3/2-1/2}\sim 0$. Therefore, $A_y(\theta)$ is proportional to $9\Delta_{5/2-3/2}$ ($4\Delta_{3/2-1/2}$) for W_a (the other 3NF models). The difference of the factors, 9 and 4, explains the reason why W_a gives a large increase in $A_y(\theta)$ in spite of the same order of the phase shift differences, $\Delta_{5/2-3/2}$ and $\Delta_{3/2-1/2}$. However, the difference seems to affect incorrectly the deuteron tensor analyzing powers.

In summary, we have studied the effects of the 2πE-3NF, and its variations, on some observables for n-d elastic scattering at low energy. We found that a contact term included in the 2πE-3NF gives a rather large $A_y(\theta)$ effect. This is the reason why the effects on $A_y(\theta)$ by BR/TM-3NF are different from those by BR$'$/UR-3NF, which does not include the contact term. $A_y(\theta)$ increases by about 5% with a 2πE-3NF model in which the contact term is eliminated. However, this increase is essentially the result of a decrease in the differential cross section caused by reproducing the triton binding energy. This contrasts with the increase of $A_y(\theta)$ by the modification of the ^3P_J NN force, which is caused by a variation in spin-dependent cross sections. We found a phenomenological 3NF model which reproduces both of the triton binding energy and $A_y(\theta)$. This 3NF originates from πN S wave scattering in the intermediate state with the strength parameter adjusted to reproduce the triton binding energy. But this 3NF destroys the good fit of the tensor analyzing power at the same time. Since forces arising from the exchange of pions should have a tensor character, it seems natural that such forces affect not only the spin vector observables but also the spin tensor observables. A 3NF involving any mechanism other than 2πE, which might have a character of a spin-orbit forces as suggested from the modification of the ^3P_J NN force, should be examined to resolve the $A_y(\theta)$ puzzle.

Appendix. In the spherical base, $A_y(\theta)$ is given by

$$I(\theta)A_y(\theta)=iI(\theta)(T_{+1}(\theta)+T_{-1}(\theta))/\sqrt{2}, \qquad (4)$$

with $I(\theta)=\text{Tr}(MM^\dagger)$, and $I(\theta)T_\kappa(\theta)=\text{Tr}(M\tau_\kappa^1 M^\dagger)$, where

M is a transition matrix and τ_κ^1 is a nucleon rank-1 spin operator, whose matrix elements in the channel-spin representation are

$$\langle s\nu|\tau_\kappa^1|s'\nu'\rangle=(-1)^{2s+(1/2)-\nu'}\sqrt{2}\hat{s}\hat{s}'$$
$$\times(ss'-\nu\nu'|1-\kappa)\begin{Bmatrix} s & s' & 1 \\ 1/2 & 1/2 & 1 \end{Bmatrix}. \qquad (5)$$

Here, $\hat{n}=\sqrt{2n+1}$, and s is the channel-spin.

With partial-wave amplitudes, $M_{sls'l'}^J$, the transition matrix elements, $M_{s\nu s'\nu'}$, are given as [30]

$$M_{s\nu s'\nu'}(\theta)=\sum_{J,l,l',m_l}\hat{l}'(sl\nu m_l|J\nu')$$
$$\times(s'l'\nu'0|J\nu')M_{sls'l'}^J Y_l^{m_l}(\theta,0). \qquad (6)$$

Here, we apply some assumptions.

(i) We assume off-diagonal matrix elements of the partial wave amplitude vanish:

$$M_{sls'l'}^J=\delta_{s,s'}\delta_{l,l'}M_{2s+1l_J}. \qquad (7)$$

(ii) Since we are interested in ^4P_J waves, we consider contributions only from $s=3/2$. Then we have

$$I(\theta)T_\kappa(\theta)=4\sum_{\nu,\nu',\nu''}(-1)^{-1/2-\nu'}M_{\nu\nu'}M_{\nu\nu''}^*$$
$$\times\left(\frac{3}{2}\frac{3}{2}-\nu'\nu''|1-\kappa\right)\begin{Bmatrix} 3/2 & 3/2 & 1 \\ 1/2 & 1/2 & 1 \end{Bmatrix}, \qquad (8)$$

with

$$M_{\nu\nu'}(\theta)=\sum_{J,l,m_l}\hat{l}\left(\frac{3}{2}l\nu m_l|J\nu'\right)\left(\frac{3}{2}l\nu'0|J\nu'\right)$$
$$\times M_{4l_J}Y_l^{m_l}(\theta,0), \qquad (9)$$

$$M_{\nu\nu''}^*(\theta)=\sum_{J',l',m_l'}\hat{l}'\left(\frac{3}{2}l'\nu m_l'|J'\nu''\right)\left(\frac{3}{2}l'\nu''0|J'\nu''\right)$$
$$\times M_{4l_J'}^* Y_{l'}^{m_l'*}(\theta,0). \qquad (10)$$

(iii) It is noted that the shape of $I(\theta)A_y(\theta)$ for the n-d scattering is roughly given by $\sin\theta$. This θ dependence arises when $(l,m_l,l',m_l')=(1,\pm1,0,0)$, or $(0,0,1,\pm1)$. For these cases, after evaluating the summation over ν, ν' and m_l in Eq. (8), we obtain

$$I(\theta)T_\kappa(\theta)\propto\kappa Y_1^\kappa(\theta,0)M_{4S_{1/2}}^*\sum_J M_{4P_J}$$
$$\times(-1)^{J-1/2}\hat{J}^2\begin{Bmatrix} 1 & 1 & 1 \\ 3/2 & 3/2 & J \end{Bmatrix}. \qquad (11)$$

The summation in Eq. (11) is proportional to Eq. (2).

[1] W. Glöckle, H. Witała, D. Hüber, H. Kamada, and J. Golak, Phys. Rep. **274**, 107 (1996).

[2] Y. Koike and J. Haidenbauer, Nucl. Phys. **A463**, 365c (1987).

[3] H. Witała, W. Glöckle, and T. Cornelius, Nucl. Phys. **A491**, 157 (1988).

[4] J. E. McAninch, L. O. Lamm, and W. Haeberli, Phys. Rev. C **50**, 589 (1994).

[5] V. G. J. Stokes, R. A. M. Klomp, C. P. F. Terheggen, and J. J. de Swart, Phys. Rev. C **49**, 2950 (1994).

[6] R. B. Wiringa, V. G. J. Stokes, and R. Schiavilla, Phys. Rev. C **51**, 38 (1995).

[7] R. Machleidt, F. Sammarruca, and Y. Song, Phys. Rev. C **53**, R1483 (1996).

[8] H. Witała and W. Glöckle, Nucl. Phys. **A528**, 48 (1991).

[9] T. Takemiya, Prog. Theor. Phys. **86**, 975 (1991).

[10] W. Tornow, H. Witała, and A. Kievsky, Phys. Rev. C **57**, 555 (1998).

[11] P. Doleschall, Few-Body Syst. **23**, 149 (1998).

[12] H. Witała, W. Glöckle, and T. Takemiya, Prog. Theor. Phys. **88**, 1015 (1992).

[13] D. Hüber and J. L. Friar, Phys. Rev. C **58**, 674 (1998).

[14] W. Tornow and H. Witała, Nucl. Phys. **A637**, 280 (1998).

[15] S. A. Coon, M. D. Scadron, P. C. McNamee, B. R. Barrett, D. W. E. Blatt, and B. H. J. McKellar, Nucl. Phys. **A317**, 242 (1979); S. A. Coon and W. Glöckle, Phys. Rev. C **23**, 1790 (1981).

[16] H. T. Coelho, T. K. Das, and M. R. Robilotta, Phys. Rev. C **28**, 1812 (1983).

[17] M. R. Robilotta and H. T. Coelho, Nucl. Phys. **A460**, 645 (1986).

[18] H. Witała, D. Hüber, and W. Glöckle, Phys. Rev. C **49**, R14 (1994).

[19] S. Ishikawa, Y. Wu, and T. Sasakawa, *Proceedings of the Few-Body Problems in Physics*, Williamsburg, VA, 1994, edited by F. Gross, AIP Conf. Proc. 334 (AIP, New York, 1995), p. 840.

[20] A. Kievsky, M. Viviani, and S. Rosati, Phys. Rev. C **52**, R15 (1995).

[21] A. Kievsky, S. Rosati, W. Tornow, and M. Viviani, Nucl. Phys. **A607**, 402 (1996).

[22] J. Fujita and H. Miyazawa, Prog. Theor. Phys. **17**, 360 (1957).

[23] P. Schwarz, H. O. Klages, P. Doll, B. Haesner, J. Wilczynski, B. Zeitnitz, and J. Kecskemeti, Nucl. Phys. **A398**, 1 (1983).

[24] T. Sasakawa and S. Ishikawa, Few-Body Syst. **1**, 3 (1986).

[25] S. Ishikawa, Nucl. Phys. **A463**, 145c (1987).

[26] T. Sasakawa, Phys. Rev. C **17**, 2015 (1978).

[27] Y. Koike and Y. Taniguchi, Few-Body Syst. **1**, 13 (1986).

[28] J. L. Friar, D. Hüber, and U. van Kolck, Phys. Rev. C **59**, 53 (1999).

[29] S. Shimizu, K. Sagara, H. Nakamura, K. Maeda, T. Miwa, N. Nishimori, S. Ueno, T. Nakashima, and S. Morinobu, Phys. Rev. C **52**, 1193 (1995).

[30] R. G. Seyler, Nucl. Phys. **A124**, 253 (1969).